International Journal of Multidisciplinary Innovative Research
Volume 6, Number 3 (July' 2026) pp. 1–7
DOI: https://doi.org/10.66566/ijmir/2026.v6n3.01
ISSN: 2583-0228
https://www.ijmir.org

Received: 13 Mar' 2026 | Revised: 01 May' 2026 | Accepted: 08 May' 2026 | Published: 01 July' 2026

Review Article

OPEN ACCESS

First-Principles Investigation on the Impact of Electric Fields on the Electronic Properties of Monolayer SiS and SiS_2 for Nanoelectronic Applications

Vu Khac Hung, Duong Thi Loan and Le Nhat Bang*

Faculty of Technology and Engineering, Thai Binh University, Hung Yen, Vietnam.

*Email: vuonthebang@gmail.com**

Abstract: *In this study, the structural and electronic properties of monolayer SiSx (x = 1, 2) and the influence of external electric fields were systematically investigated using first-principles density functional theory (DFT) calculations. The computed results reveal that both monolayer SiS and SiS2 are indirect-gap semiconductors with band gaps of approximately 3.0 eV and 2.2 eV, respectively, as determined using the HSE06 hybrid functional. Notably, the application of an external electric field can effectively and continuously modulate the electronic band structure and band gap of both materials, demonstrating strong potential for field-tunable electronic and optoelectronic devices. These findings not only deepen our understanding of the fundamental electronic properties of SiS-based monolayers but also provide essential theoretical guidance for their exploitation in next-generation nanoelectronic and optoelectronic technologies.*

Keywords: *Band Gap, Semiconductors, Electric Field, Density Functional Theory, Monolayer Structures.*

INTRODUCTION

Two-dimensional (2D) materials with monolayer structures have emerged as a central research focus in condensed matter physics, materials science, and modern electronics, owing to their extraordinary physical and chemical properties that are absent in their bulk counterparts. Since the pioneering synthesis and characterization of graphene by Novoselov et al. [1], the field of 2D materials has experienced rapid expansion. These atomically thin structures have been recognized as promising platforms for a broad spectrum of advanced applications, including optical sensors, supercapacitors, piezoelectric nanogenerators, artificial muscles, and nanoelectronic devices [2, 3]. Beyond graphene, numerous other 2D materials-such as molybdenum disulfide (MoS_2), hexagonal boron nitride (*h*-BN), titanium dioxide (TiO_2), and zinc oxide (ZnO)-have been extensively investigated for their distinctive optical, thermal, electronic, and catalytic properties [4–7]. Among the growing family of 2D materials, silicon monosulfide (SiS) and silicon disulfide (SiS_2) have attracted considerable attention due to their promising electronic and optoelectronic characteristics.

Ullah et al. demonstrated that monolayer SiS exhibits a small lattice mismatch (~0.3%) with silicon substrates and a higher electron mobility compared to hole mobility, which facilitates efficient electron–hole separation and enhances overall device performance [8]. From a thermoelectric perspective, Elsalam reported that the Seebeck coefficient of monolayer SiS increases with temperature, while its electrical and electronic thermal conductivities decrease, suggesting significant prospects for optimizing thermoelectric efficiency [9]. In parallel, Guan et al. established that monolayer SiS_2 behaves as an indirect semiconductor [10], and Bera revealed that SiS_2 possesses an exceptionally high Seebeck coefficient in the range of 2100–2281 μV/K together with a large thermoelectric power factor at 300 K [11], further underscoring its potential for energy-harvesting applications.

Despite these significant advances, a comprehensive understanding of the tunability of the electronic band structure of SiS and SiS_2 monolayers under external perturbations-particularly applied electric fields-remains limited. Electric-field engineering represents a powerful, non-invasive strategy for modulating the electronic properties of 2D semiconductors without altering their chemical composition, and is directly applicable in field-effect transistor (FET) architectures.

In this work, first-principles DFT calculations are employed to systematically examine the structural stability and electronic properties of monolayer SiS and SiS_2, with particular emphasis on the tunability of the band gap under externally applied electric fields ranging from −10.0 to +10.0 V/nm. The present results provide quantitative theoretical insights into the field-induced band-gap modulation of these materials and are expected to guide their future development in reconfigurable nanoelectronic and optoelectronic applications.

COMPUTATIONAL DETAILS

All first-principles calculations were performed within the framework of density functional theory (DFT) as implemented in the Quantum ESPRESSO (QE) package [12]. The exchange–correlation energy was treated using the generalized gradient approximation (GGA) in the Perdew–Burke–Ernzerhof (PBE) parameterization [13]. Ultrasoft pseudopotentials were employed to describe the electron–ion interactions. The Kohn–Sham wave functions and the charge density were expanded in plane-wave basis sets with kinetic energy cutoffs of 60 Ry and 600 Ry, respectively. Brillouin zone integrations were performed using a Γ-centered 15×15×1 k-point mesh generated according to the Monkhorst–Pack scheme [14]. To prevent spurious interlayer interactions under the periodic boundary conditions imposed along the out-of-plane direction, a vacuum spacing of 30 Å was inserted along the *z*-axis.

Structural optimization was conducted at 0°K until the Hellmann–Feynman forces on each atom were smaller than 5×10^{-3} Ry/a.u. and the residual stress was below 5×10^{-2} GPa, ensuring fully converged equilibrium geometries. To correct for the well-known underestimation of band gaps within the GGA–PBE functional, the Heyd–Scuseria–Ernzerhof (HSE06) screened hybrid functional [15] was subsequently applied to refine the electronic band structure calculations.

Band interpolation and Wannier-function-based corrections were carried out using the Wannier90 code [16]. The combination of PBE-level structural optimization and HSE06-level electronic structure calculations ensures an accurate and computationally tractable description of the structural and electronic properties of monolayer SiS and SiS_2. The external electric field was applied perpendicular to the monolayer plane (along the z-axis) with magnitudes ranging from −10.0 to +10.0 V/nm.

RESULT AND DISCUSSION

Crystal Structure and Structural Optimization

Figure 1 presents the optimized atomic structures of monolayer SiS and SiS_2 in their top and side views. In the SiS monolayer, each primitive unit cell contains one Si atom and one S atom arranged in a buckled honeycomb-like configuration, whereas the SiS_2 monolayer comprises one Si atom covalently bonded to two S atoms in a trigonal planar or distorted tetrahedral environment, analogous to other group-IV dichalcogenide structures. Structural optimization at 0 K yields equilibrium lattice parameters of $a = b = 3.309$ Å with a buckling height of $h = 1.33$ Å for SiS, and $a = b = 3.28$ Å with $h = 2.68$ Å for SiS_2. These values are in good agreement with previously reported theoretical results [17], thereby validating the accuracy of the computational approach employed in this work.

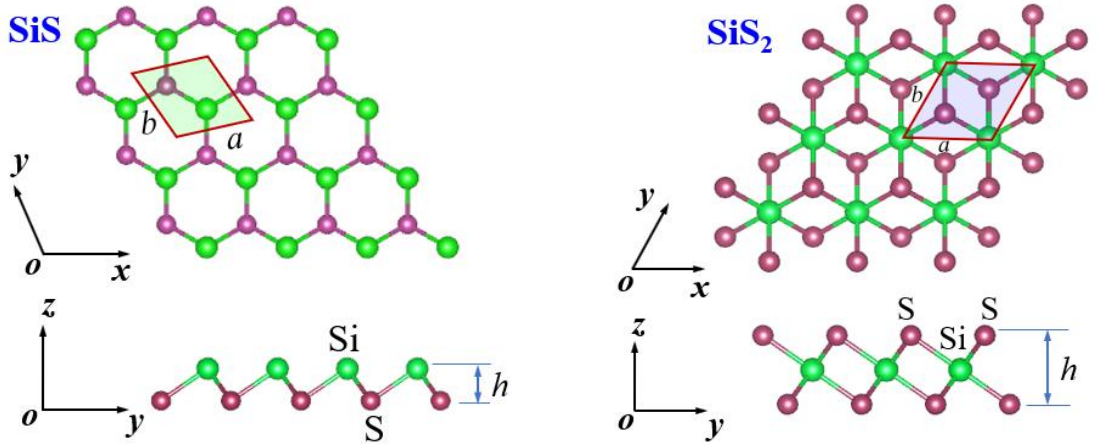

(a) (b)

Figure 1: Optimized atomic structure of monolayer (a) SiS and (b) SiS_2. Silicon (Si) and sulfur (S) atoms are represented by yellow and blue spheres, respectively. Top and side views are shown.

Electronic Band Structure at Equilibrium

Figure 2 presents the electronic band structures of monolayer SiS and SiS_2 ated at the HSE06 level under equilibrium conditions (i.e., in the absence of an external electric field). The band gap is defined as the energy difference between the valence band maximum (VBM) and the conduction band minimum (CBM). The calculations reveal that SiS exhibits a band gap of approximately 3.0 eV, while SiS_2 possesses a smaller band gap of approximately 2.2 eV. Both values are in good agreement with previously reported theoretical and experimental results [17, 18, 19]. The difference in band gap magnitudes between the two materials can be attributed to the distinct bonding environments and degree of orbital hybridization: the additional Si–S bond in SiS_2 introduces additional anti-bonding states near the band edges, thereby narrowing the gap.

Both SiS and SiS_2 are identified as indirect-gap semiconductors. In the case of SiS, the CBM is located at the high-symmetry K point, while the VBM lies along the K–Γ high-symmetry path. For SiS_2, the CBM is situated at the Γ point and the VBM is found along the Γ–M path. Such indirect-gap characteristics are commonly observed in many two-dimensional group-IV monochalcogenide and dichalcogenide semiconductors, and are associated with reduced radiative recombination rates that may, in certain contexts, be advantageous for carrier-lifetime-dependent applications.

For reference, several related 2D semiconductors exhibit moderate band gaps: $PbSe_2$ (~1.85–1.9 eV), GeS (~1.7–1.9 eV), and SnS (~1.4–1.5 eV), depending on the calculation method and layer thickness [20–22]. The comparatively wider band gaps of SiS and SiS_2 indicate strong potential for applications in high-energy photon absorption, ultraviolet photodetectors, and high-frequency optoelectronic systems. In particular, the wide band gaps confer strong photon absorption capabilities, making both monolayers promising candidates for high-performance optical sensors and photovoltaic cells.

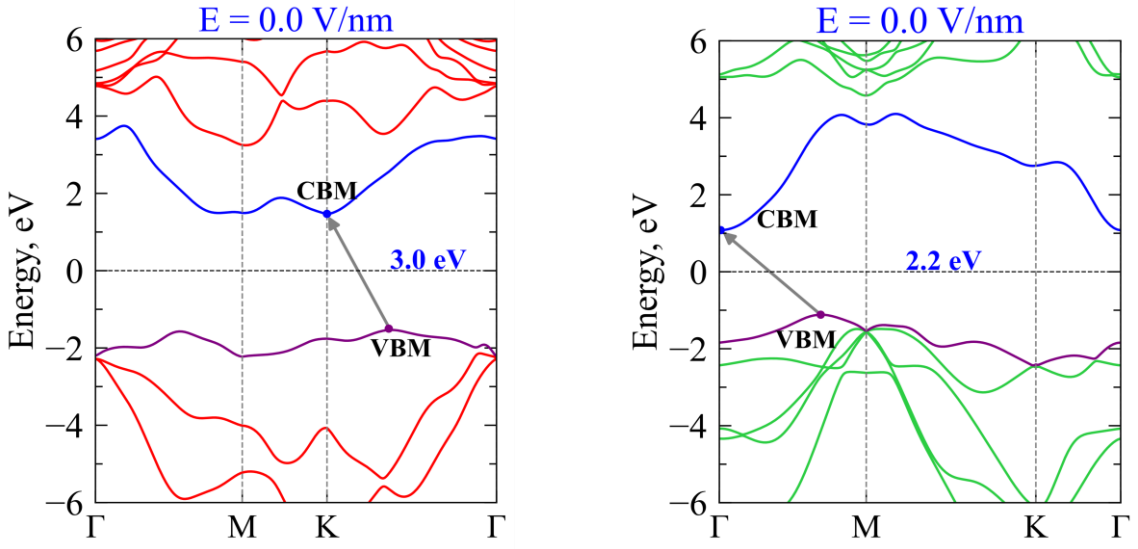

Figure 2: Electronic band structures of monolayer (a) SiS and (b) SiS_2 computed at the HSE06 level under equilibrium conditions. The Fermi level is set to zero. The red arrows indicate the indirect band gaps.

Band-Gap Modulation by External Electric Fields

To evaluate the potential of monolayer SiS and SiS_2 for field-effect electronic applications, the band structures of both materials were calculated under external perpendicular electric fields (E) ranging from −10.0 to +10.0 V/nm. Figure 3 illustrates the evolution of the band structures for representative field strengths of E = 0.0, 2.0, 4.0, 6.0, and 8.0 V/nm for both materials. The results demonstrate significant field-induced shifts in the positions and energies of the band extrema.

For monolayer SiS (Figure 3a), when the electric field increases from 0.0 to 4.0 V/nm, the positions of the CBM (at the K point) and VBM (along the K–Γ path) remain essentially unchanged, indicating that the indirect nature of the band gap is preserved at moderate field strengths. However, as E exceeds 4.0 V/nm, a notable shift of the CBM from the K point to the Γ point is observed, while the VBM remains at its original position. This field-induced relocation of the CBM modifies the band dispersion near the conduction band edge and could affect effective masses and carrier transport properties.

For monolayer SiS_2 (Figure 3b), a more complex field-dependent behavior is observed: as E increases from 0.0 to 4.0 V/nm, the CBM shifts from the Γ point to the M point, while the VBM undergoes only minor displacements along the Γ–M path. When E exceeds 4.0 V/nm, the CBM returns to the Γ point, with the VBM remaining largely unaffected. The non-monotonic response of SiS_2 to the electric field can be attributed to competition between different conduction band valleys whose relative energies are sensitively altered by the applied field.

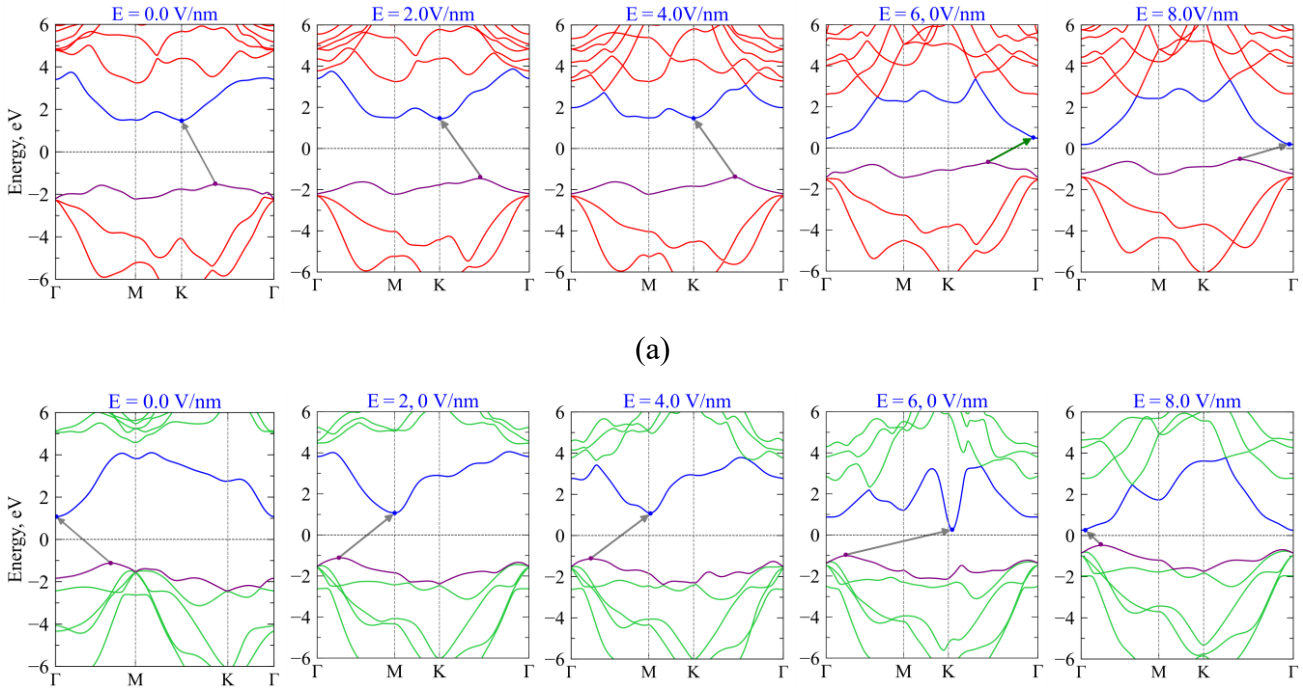

Figure 3: Evolution of the electronic band structure of (a) monolayer SiS and (b) monolayer SiS_2 under external electric field strengths of E = 0.0, 2.0, 4.0, 6.0, and 8.0 V/nm.

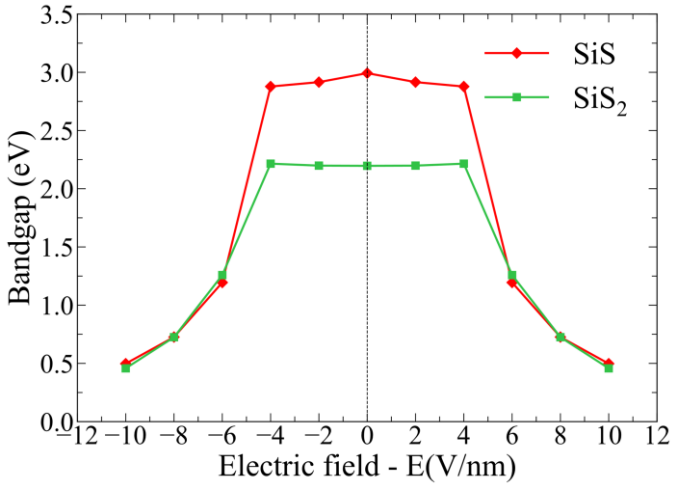

Figure 4: Variation of the electronic band gap of monolayer SiS and SiS_2 as a function of the applied external electric field strength (E).

Figure 4 quantitatively illustrates the variation in the band gap of monolayer SiS and SiS_2 as a function of the applied electric field magnitude. Both materials exhibit a broadly similar field-dependent trend, with the band gap generally decreasing as the electric field intensity increases, consistent with the quantum-confined Stark effect commonly observed in low-dimensional semiconductor systems. For $E \leq \pm 4.0$ V/nm, the band gap of SiS_2 remains nearly constant, whereas that of SiS decreases gradually, reflecting the different sensitivities of the two materials to external fields. At $E = \pm 6.0$ V/nm, the band gaps of both SiS and SiS_2 are significantly reduced to 60% and 42.6% of their respective equilibrium values, indicating a

pronounced and practically useful field-induced modulation. At the higher field strength of $E = \pm 10.0$ V/nm, the reductions become even more dramatic, amounting to 82.7% for SiS and 79.3% for SiS_2.

These findings demonstrate that both monolayers possess highly responsive and tunable electronic properties under applied electric fields. The ability to continuously reduce the band gap from ~3.0 eV (SiS) and ~2.2 eV (SiS_2) to substantially smaller values without structural disruption highlights the strong potential of these materials for applications in field-effect transistors (FETs), reconfigurable logic circuits, electric-field-controlled photodetectors, and non-volatile information storage systems. Compared with other representative 2D semiconductors such as $PbSe_2$ and SnS, monolayer SiS and SiS_2 exhibit greater initial band gaps and comparable-or superior-tunability, offering a wider operational window for field-tunable optoelectronic devices. Furthermore, the present results suggest new research directions in band engineering of 2D materials for photovoltaic and photocatalytic applications, where precise control over the optical absorption edge is essential.

CONCLUSION

In this study, the structural and electronic properties of monolayer SiS and SiS_2 were systematically investigated using first-principles density functional theory calculations with the HSE06 hybrid functional. The key findings can be summarized as follows. First, both monolayer SiS and SiS_2 are confirmed to be indirect-gap semiconductors, with equilibrium band gaps of approximately 3.0 eV and 2.2 eV, respectively. These wide band gaps, combined with strong photon absorption characteristics, render both materials highly promising candidates for high-performance optical sensors, ultraviolet photodetectors, and photovoltaic cells. Second, the application of an external perpendicular electric field enables effective and continuous modulation of the band gaps of both materials. At moderate field strengths ($E = \pm 6.0$ V/nm), the band gaps are reduced to approximately 60% (SiS) and 42.6% (SiS_2) of their equilibrium values, while at $E = \pm 10.0$ V/nm, reductions of 82.7% and 79.3% are achieved, respectively. Third, field-induced shifts in the band-edge k-point positions are observed for both materials, suggesting tunability not only of the gap magnitude but also of the carrier effective masses and transport properties. Taken together, these results underscore the exceptional potential of monolayer SiS and SiS_2 as versatile, field-tunable semiconductors for next-generation nanoelectronic and optoelectronic device technologies, including field-effect transistors, reconfigurable logic circuits, and field-controlled data storage systems.

AKNOWLEDGEMENT

This research was funded by the Scientific Project under Code: ĐHTB-ĐT01/25-26.

REFERENCES

[1] K. S. Novoselov *et al.*, "Electric field effect in atomically thin carbon films," *Science*, vol. 306, no. 5696, pp. 666–669, Oct. 2004.

[2] V. A. Cao *et al.*, "Enhanced piezoelectric output performance of the SnS2/SnS heterostructure thin-film piezoelectric nanogenerator realized by atomic layer deposition," *ACS Nano*, vol. 15, no. 2, pp. 10428–10436, Feb. 2021.

[3] L. Zhang *et al.*, "Design, synthesis, and application of some two-dimensional materials," *Chem. Sci.*, vol. 14, no. 3, pp. 5266–5290, 2023.

[4] M. Ye *et al.*, "Recent advancement on the optical properties of two-dimensional molybdenum disulfide (MoS2) thin films," *Photonics*, vol. 2, no. 1, pp. 288–307, 2015.

[5] V. Guerra *et al.*, "Thermal conductivity of 2D nano-structured boron nitride (BN) and its composites with polymers," *Prog. Polym. Sci.*, vol. 100, p. 170186, Jan. 2020.

[6] S. Çeşmeli and C. Biray Avci, "Application of titanium dioxide (TiO2) nanoparticles in cancer therapies," *J. Drug Target.*, vol. 27, no. 6, pp. 762–766, 2019.

[7] D. M. Cruz *et al.*, "Green nanotechnology-based zinc oxide (ZnO) nanomaterials for biomedical applications: a review," *J. Phys. Mater.*, vol. 3, no. 3, p. 034005, Jun. 2020.

[8] S. Ullah *et al.*, "First-principles study of the electronic structures and optical and photocatalytic performances of van der Waals heterostructures of SiS, P and SiC monolayers," *RSC Adv.*, vol. 11, no. 24, pp. 14263–14268, 2021.

[9] M. Elsalam, "Thermoelectric properties of monolayer silicon monosulfide (SiS)," [Full citation details missing], n.d.

[10] Y. Guan *et al.*, "Tunable electronic properties of type-II SiS_2/WSe_2 hetero-bilayers," *Appl. Sci.*, vol. 10, no. 17, p. 2037, Aug. 2020.

[11] J. Bera, "Thermoelectric properties of monolayer silicon disulfide (SiS_2)," [Full citation details missing], n.d.

[12] P. Giannozzi *et al.*, "QUANTUM ESPRESSO: a modular and open-source software project for quantum simulations of materials," *J. Phys.: Condens. Matter*, vol. 21, no. 39, p. 395502, Sep. 2009.

[13] J. P. Perdew, K. Burke, and M. Ernzerhof, "Generalized gradient approximation made simple," *Phys. Rev. Lett.*, vol. 77, no. 18, pp. 3865–3868, Oct. 1996.

[14] H. J. Monkhorst and J. D. Pack, "Special points for Brillouin-zone integrations," *Phys. Rev. B*, vol. 13, no. 12, pp. 5188–5192, Jun. 1976.

[15] J. Heyd, G. E. Scuseria, and M. Ernzerhof, "Hybrid functionals based on a screened Coulomb potential," *J. Chem. Phys.*, vol. 118, no. 18, pp. 8207–8215, May 2003.

[16] A. A. Mostofi *et al.*, "An updated version of Wannier90: A tool for obtaining maximally-localised Wannier functions," *Comput. Phys. Commun.*, vol. 185, no. 8, pp. 2309–2310, Aug. 2014.

[17] Q. Alam *et al.*, "First-principles study of the electronic structures and optical and photocatalytic performances of van der Waals heterostructures of SiS, P and SiC monolayers," *RSC Adv.*, vol. 11, no. 24, pp. 14263–14268, 2021.

[18] W. J. Zhao *et al.*, "First-principles study on the photocatalytic property of SiS/BSe and SiS2/BSe van der Waals heterojunctions," *Eur. Phys. J. B*, vol. 96, no. 7, pp. 92–102, Jul. 2023.

[19] Y. Guan *et al.*, "Tunable electronic properties of type-II SiS2/WSe2 hetero-bilayers," *Appl. Sci.*, vol. 10, no. 17, p. 2037, Aug. 2020.

[20] Y. Mao *et al.*, "Tunable optoelectronic properties of two-dimensional PbSe by strain: First-principles study," *Comput. Mater. Sci.*, vol. 202, p. 110957, Feb. 2022.

[21] N. T. Kaner *et al.*, "Enhanced shift currents in monolayer 2D GeS and SnS by strain-induced band gap engineering," *ACS Omega*, vol. 5, no. 28, pp. 17207–17214, Jul. 2020.

[22] C. Xia *et al.*, "A type-II GeSe/SnS heterobilayer with suitable direct gap, superior optical absorption and broad spectrum for photovoltaic applications," *J. Mater. Chem. A*, vol. 5, no. 26, pp. 13400–13410, 2017.